Transportation Research Part B 153 (2021) 111–127

Contents lists available at ScienceDirect

Transportation Research Part B

journal homepage: www.elsevier.com/locate/trb

Vulnerability analysis of cut-capacity structure and OD demand using Gomory-Hu tree method

Satoshi Sugiura [a,*], Anthony Chen [b]

[a] Graduate School of Engineering, Hokkaido University, Kita 13, Nishi 8, Kita-ku, Sapporo, Hokkaido, Japan
[b] Department of Civil and Environmental Engineering, Hong Kong Polytechnic University, Hung Hom, Kowloon, Hong Kong

ARTICLE INFO

Keywords:
Network vulnerability
Connectivity analysis
Minimum cut
Gomory–Hu tree

ABSTRACT

Vulnerability analysis of transportation networks has rapidly become important in recent decades given the increasing numbers of transportation disasters. In this paper, we describe a method for calculating the minimum cuts between all pairs of nodes in a transportation network and develop two indices for analyzing vulnerability; these are derived from topology-based vulnerability/demand-accountable analyses and enable evaluation of cuts without assuming route-choice behaviors. We show that such analyses can be performed using a Gomory–Hu tree to reduce the computational load. This method is efficient, requiring only $N-1$ calculations of the maximum flow problem even though the number of node pairs is N^2, where N is the number of nodes. In addition, we show that the total demand passing each minimum cut, which is necessary for demand-accountable analysis, can be obtained by network loading onto the tree using the Gomory–Hu tree features. We apply the proposed method to the central region of Japan to illustrate the applicability of the two indices for identifying vulnerable links in the road network.

1. Introduction

1.1. Importance of vulnerability analysis in transportation networks

Vulnerability analysis in transportation networks allows analyzing the impacts of degradation of the network components (Berdica, 2002; Faturechi and Miller-Hooks, 2015); it is one of the important topics in transportation research in the past few decades owing to the increasing number of disasters. A brief discussion on the concept of vulnerability and review of related studies are given in Taylor (2017) and Mattsson and Jenelius (2015). Similar to vulnerability, reliability analysis is a concept that focuses on the risk of performance degradation due to network degradation. Reliability analysis generally considers the probability of network component failures, whereas vulnerability analysis excludes such probability from consideration by focusing only on the impact of failure (Jenelius et al., 2006). Vulnerability analysis is thus appropriate for a small probability of failure or for external forces that are not easy to estimate but have large impacts on society (e.g., earthquakes, attacks on human) (Taylor, 2017). Vulnerability analysis provides valuable information for disaster prevention planning by analyzing the impact of network degradation. Many vulnerability analysis methods provide measures to find network components whose degradations have greater impacts; once these vulnerable components are identified, various reinforcement schemes can be implemented to mitigate or eliminate disruptions from external forces. Numerous vulnerability studies have provided measures to estimate the impacts of component failures, allowing analyses based on various

* Corresponding author.
E-mail address: sugiura@eng.hokudai.ac.jp (S. Sugiura).

https://doi.org/10.1016/j.trb.2021.08.013
Received 30 December 2020; Received in revised form 19 April 2021; Accepted 29 August 2021
Available online 25 September 2021

Table 1
Organization of required performances for the road network (Tatano, 2017).

Time elapsed after disaster	Phase of disaster response	Measures (example)
Few days	Critical care	Connectivity to the center hospital
Few months	Relief	Connectivity and travel time from disaster centers to evacuation centers
Several months	Recovery	Network capacity, Consumer surplus
Few years	Continuation/ reconstruction of economic activities	Network capacity, Consumer surplus

perspectives. Taylor (2017) referred to the concept of vulnerability defined by Berdica (2002) and D'Este and Taylor (2001, 2003), and noted that definitions based on serviceability are useful for measuring impact in the short term (hours-days-weeks) and definitions based on accessibility are useful for considering socioeconomic impacts in the long term (weeks-month-years), respectively. Tatano (2017) summarized the relationship between specific post-disaster phases and the performance required of transportation networks as shown in Table 1. Accordingly, the network administrator is required to prepare for transportation network failure from a single external force by evaluating each index depending on the required performance from the network during each phase after disaster occurrence. Given this property, the vulnerability indices should be applied in a manner consistent with the functioning of the road network, as required under the disaster situation.

We categorized the literature on vulnerability analysis according to the phases shown in Table 1. During the recovery and continuation phases, the road networks must cope with different traffic demands. If network capacity is reduced even slightly by an external force, recovery from a disaster may be delayed. When evaluating these phases, an indicator of the overall network performance is desirable. A typical index is the total travel time, as suggested by Bell (2000), Murray-Tuite and Mahmassani (2004), Jenelius et al. (2006) and Scott et al. (2006). Nagurney and Qiang (2007) defined the network efficiency measure that accounts for demand and equilibrium disutility. The reserve capacity concept was investigated by Wong and Yang (1997), as it can indicate the serviceability of a road network. Chen and Kasikitwiwat (2011) used the network capacity concept to analyze the capacity flexibility of a transportation system, while Bell et al. (2017) and Du et al. (2017) analyzed the capacity vulnerabilities of road networks.

Road network phases close to disaster occurrences are required to connect two arbitrary nodes with strong connectivities. The main index used to evaluate connectivity between two such nodes is accessibility (D'Este and Taylor, 2003; Chen et al., 2007; Taylor, 2008; Taylor and Susilawati, 2012; Ho et al., 2013). The accessibility index can also consider network serviceability by aggregating the obtained accessibility values for the entire network. Another method to evaluate connectivity is by directly counting the number of paths between two given nodes (Kurauchi et al., 2009; Xu et al., 2018). Matisziw and Murray (2009) discussed the number of disconnected origin–destination (OD) pairs as a vulnerability indicator by removing the links in the network. These methods only focus on the network topology and do not consider OD flow, which has been classified for topological vulnerability analysis by Mattsson and Jenelius (2015). The present study considers vulnerability of network connectivity required for a phase very close to a disaster and addresses the connectivity between two nodes in the network to find the vulnerable components.

1.2. Objective and contributions

The existence of flow bottlenecks in transportation networks is an important factor determining vulnerability. Locations where large demands routinely flow into small capacity bottlenecks can cause significant disruptions in the event of network failure. The relationships between amount of flow and capacity of a single link have been analyzed through the concept of reserve capacity. Methods for analyzing reserve capacity over a wide range of networks and identifying vulnerable links have been considered by Wong and Yang (1997) and Chen and Kasikitwiwat (2011). In this study, we provide a methodology that focuses not on a single link but on the cuts that contain multiple links to partition the network. If the capacity of the cut that separates the network (i.e., total capacity of the links contained in the cut) is small, then the connectivity is considered potentially vulnerable. Conversely, if the capacity of a cut is large and if the flow through the cut is larger, then such a location is also considered a bottleneck and is potentially vulnerable. For disaster prevention planning, finding a vulnerable cut (i.e., multiple links that separate the OD pairs) sometimes has the obvious advantage over finding just a single critical link. If regional evacuation is required (e.g., after an earthquake, nuclear accident, or volcanic eruption), the cut capacity of a road network reflects the probability of full evacuation within the target time. Hence, vulnerability analysis of cuts is expected to be important for disaster management planning, but not many studies have been reported on it. Bell et al. (2017) identified vulnerable cuts via spectral partitioning; this method can identify cuts without route choice proportions or route choice model. However, OD demand was not considered, which is key to disaster prevention analysis. For example, a vulnerable cut with small crossing demand may not need reinforcing investment in terms of cost-effectiveness; however, a large demand would need maintenance or rapid reinforcement.

We describe a method to calculate the minimum cuts between all pairs of nodes in a transportation network, and develop two indices for analyzing vulnerability for each of the minimum cuts. The proposed method can be categorized into the connectivity evaluation approach that aims to evaluate serviceability in the phase close to disaster occurrence. While the proposed index is a topology-based vulnerability index, it allows consideration of the demand. We show that such analyses can be performed using a Gomory–Hu tree (Gomory and Hu, 1961) to reduce the computational load. This method is efficient, requiring only $N-1$ the calculations of the maximum flow problem (MFP) despite the number of node pairs being N^2, where N is the number of nodes. Such

Table 2
Notations used in the methodology.

Notation	Description
V	Set of nodes in the network, the elements of $n \in V$
A	Set of links in the network
$G(V, A)$	Network consisting of node set $V$and link set A
a	A link in the network ($a \in A$)
S	Subset of nodes in the network ($S \subseteqq V$)
λ	Solution of the maximum flow problem
x_a	Flow along link a
c_a	Capacity of link a
y	Design variable for the maximum flow problem
s	Origin node ($s \in V$)
t	Destination node ($t \in V$)
$out(n)$	Set of links that exit from n
$in(n)$	Set of links that enter n
d_{st}	Demand volume from origin s to destination t
$\mathbf{X}^{(n)}$	Set of hypernodes in the tree of iteration n
X_i	Hypernode in the tree ($X_i \in \mathbf{X}^{(n)}$)
$\mathbf{E}^{(n)}$	Set of virtual links in the tree for iteration n
e_{ij}	Virtual link connecting X_i and X_j in the tree ($e_{ij} \in \mathbf{E}^{(n)}$)
$\pi_{e_{ij}}$	Weight of virtual link e_{ij}
$T_n(\mathbf{X}^{(n)},\mathbf{E}^{(n)})$	Tree consisting of hypernodes $\mathbf{X}^{(n)}$ and virtual links $\mathbf{E}^{(n)}$in the process of generating the Gomory–Hu tree
$\mathbf{a}$	Set of links consisting the minimum cuts
W	Set of OD pairs whose elements are represented as (s, t)

analysis is applicable to undirected networks, and the capacities of all links therein are obtained. Therefore, public transportation methods such as bus networks and railways can be analyzed. Herein, we use road networks to show that our proposed method can handle large-scale networks.

Thus, the main contributions of this study can be summarized as follows:

- Providing two vulnerability indicators based on the capacity of a cut; our indicators are not a single-link degradation index, but a combination of multiple links formed by the cut to represent a composite vulnerability indicator. Many existing vulnerability studies focus on a single-link degradation.
- Proposed multiple-link indicator not only considers the capacity of the cut, but also accounts for the demand passing through the cut (i.e., traffic flow on these cut links). This is an approach for adding information on demand, which is important in disaster prevention planning, to the vulnerability analysis of cuts.
- Providing the Gomory–Hu tree method to generate the minimum cuts between all two-node pairs in the network and evaluating them with the proposed two indicators. This method does not need to know the route choice proportions or a route choice model. This good feature is similar to the capacity weighted spectral partitioning method of Bell et al. (2017).
- Proof that the demand passing through each minimum cut is equal to the total flow obtained by network loading onto the Gomory–Hu tree.

We apply the proposed method to the central region of Japan to illustrate the applicability of the two indices to identify vulnerable links in the road network.

The remainder of the paper is organized as follows. Section 2 details our proposed vulnerability indices and explains the Gomory–Hu tree method to generate the minimum cuts between all pairs of nodes in the network. Section 3 shows the application of this method to analyze the vulnerability of the Chubu regional network of Japan (which has 18,051 links, 12,007 nodes, 1049 centroids, and 182,263 OD pairs). Sections 4 and 5 present the discussion and conclusions of this study.

2. Methodology

2.1. Notation

The notations used in the present study are summarized in Table 2.

2.2. Connectivity vulnerability

The solution to the MFP is often used to determine the minimum cut; this also determines the maximum flow between an arbitrary pair of s and t places in a network exhibiting link capacity constraints and is formulated as follows:

$$\lambda = \max_{x,y} y \tag{1}$$

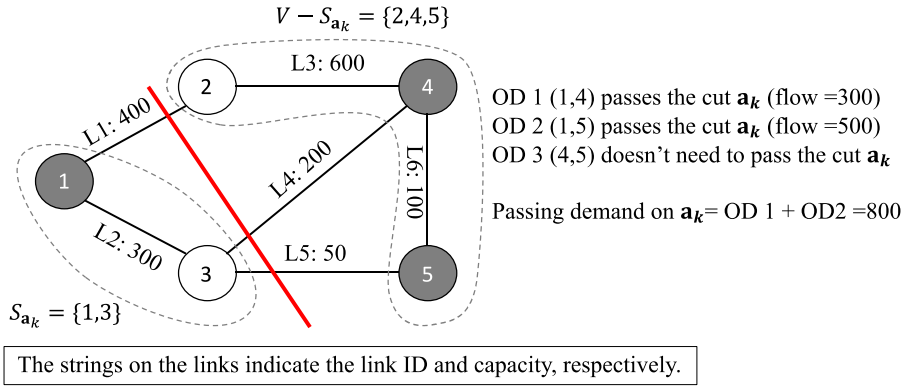

Fig. 1. Example of minimum cut and passing demand.

subject to:

$$\sum_{a\in out(s)} x_a - y = 0 \tag{2}$$

$$\sum_{a\in in(t)} x_a - y = 0 \tag{3}$$

$$\sum_{a\in in(n)} x_a - \sum_{a\in out(n)} x_a = 0,\ \forall n \in V - \{s,t\} \tag{4}$$

$$x_a \le c_a,\ \forall a \in A \tag{5}$$

$$x_a > 0,\ \forall a \in A$$

$$y \ge 0 \tag{6}$$

The MFP can be solved by linear programming methods (Goldberg and Tarjan, 1988). The minimum cut between any two nodes, according to the MFP solution, indicates the "connectivity-vulnerability" (i.e., a smaller cut indicates a larger vulnerability). The cut links are found from the MFP solution as the set of links $\{a|x_a = c_a\}$.

2.3. Capacity vulnerability

The capacity vulnerability is determined according to the demand imposed by the minimum cut. If more demand passes through the capacity of the cuts obtained by the MFP, it could pose serious problems for situations such as emergency evacuations. Therefore, we define the ratio of the passing demand to cut capacity as the capacity vulnerability, which is evaluated as

$$Capacity\ Vulnerability\ = \frac{D_{\mathbf{a}_k}}{C_{\mathbf{a}_k}} \tag{7}$$

where $\mathbf{a}_k$ denotes the minimum cut identified by indicator k, $D_{\mathbf{a}_k}$ denotes the demand passing through the cut $\mathbf{a}_k$, and $C_{\mathbf{a}_k}$ denotes the cut capacity obtained from the MFP.

The (s, t) minimum cut not only the origin and destination (s, t) but may also pass other OD demands. Thus, the demand that passes through an arbitrary cut not only considers the (s, t) demand but also needs to be observed for the demand of the entire network to pass through this cut. The following property of cuts helps to observe the entire crossing demand.

Proposition 1. *The demand to pass through any cut* $\mathbf{a}_k$ *is obtained by the following expression:*

$$D_{\mathbf{a}_k} = \sum_{i\in S_{\mathbf{a}_k}, j\in\left(V - S_{\mathbf{a}_k}\right)} d_{ij} + \sum_{i\in\left(V - S_{\mathbf{a}_k}\right), j\in S_{\mathbf{a}_k}} d_{ij} \tag{8}$$

Proof. When a set of links containing the minimum cut $\mathbf{a}_k$ are removed from a network $G(V, A)$, the network is divided into two node subsets, namely $S_{\mathbf{a}_k}$ and $V - S_{\mathbf{a}_k}$. If the origin and destination of any given OD pair (i, j) belong to either subset, i.e., $i \in S_{\mathbf{a}_k}, j \in (V - S_{\mathbf{a}_k})$ or $i \in (V - S_{\mathbf{a}_k}), j \in S_{\mathbf{a}_k}$, there is no path between the subsets of the nodes being partitioned. In other words, the OD demand (i, j) can only reach the destination by passing through one of the links contained in $\mathbf{a}_k$. Thus, the sum of the demands of the OD pairs corresponding to $i \in S_{\mathbf{a}_k}, j \in (V - S_{\mathbf{a}_k})$ or $i \in (V - S_{\mathbf{a}_k}), j \in S_{\mathbf{a}_k}$ always passes over $\mathbf{a}_k$, and the relationship in Eq. (8) provides the passing demand for a_k.□

Table 3
Example of OD demand for the example network.

OD	Origin	Destination	Demand
1	1	4	300
2	1	5	500
3	4	5	200

This property of the cut holds even if $\mathbf{a}_k$ is not the minimum cut for the OD pair (i, j), thereby allowing travel demand analysis for an arbitrary cut. It is also notable for the ability to compute travel demand without assuming any route choice models. Fig. 1 and Table 3 show examples of the relationships between the minimum cut and passing travel demands.

Consider the cut $\mathbf{a}_k = \{L1, L4, L5\}$ in Fig. 1. This is the minimum cut among (1,2), (1,4), and (1,5). The cut $\mathbf{a}_k$ divides the node set V into $S_{\mathbf{a}_k} = \{1, 3\}$ and $V - S_{\mathbf{a}_k} = \{2,4,5\}$. The origin and destination of the OD pair 1 lie in $S_{\mathbf{a}_k}$ and $V - S_{\mathbf{a}_k}$, respectively; further, there is no path between the origin and destination that does not pass through the (1, 4) minimum cut. Similarly, the origin and destination of OD pair 2 lie in two nodal subsets, and the demand must pass through the (1, 4) minimum cut. On the contrary, both the origin and destination of OD pair 3 lie in $V - S_{\mathbf{a}_k}$, and this demand does not necessarily pass through the (1, 4) minimum cut. The sum of the flows passing through the (1, 4) minimum cut is therefore 800 (OD 1: 300 + OD 2: 500) from this example.

Using the method described above, we obtain all the OD demands that must pass through the minimum cut. The capacity of the cut is vulnerable when its value is small compared to the sum of the passing demands through (1, 4). The minimum cut flow is 800 for a capacity of 650; the flow to capacity ratio is 1.23. If the demand to capacity ratio is large, then congestion should be expected during network degradation, and even a small problem may have major effects. Hence, we refer to the ratio of passing demand to minimum cut capacity ratio as the capacity vulnerability. Road managers may find that the difference between the passing demand and minimum cut capacity, as well as the ratio of the passing demand to minimum cut capacity, are useful indicators; however, we discuss only the effects of the ratio here.

2.4. Gomory–Hu tree method

To find vulnerable cuts in the network, it is necessary to enumerate the minimum cuts between all pairs of points and evaluate the two vulnerability indicators. Calculation of the minimum cut between any two network nodes usually requires N^2 calculations. However, the MFP solutions for all the node pairs in an undirected network must be less than or equal to $N - 1$. The Gomory–Hu tree uses this property to represent the minimum cut structure in the entire network as a tree through $N - 1$ times the MFP number of operations. The Gomory–Hu tree is thus defined as follows:

Definition 1. The Gomory–Hu tree $T(V, E)$ of an undirected network $G(V, A)$ is a weighted undirected spanning tree such that the following features are satisfied:

(1) The minimum cut solution between node pair (s, t) is found as the minimum weight of a link in the unique path connecting s and t in $T(V, E)$, and this link is called e^*. If there are multiple links with minimum weights in the s to t path in $T(V, E)$, any one of these links can be designated as e^*.
(2) For any node pair (s, t), the bipartition of nodes into pairs of node sets produced by removing e^* (if there are multiple candidates for e^*, this feature holds for each candidate link) from $T(V, E)$ corresponds to a minimum (s, t) cut in the original graph $G(V, A)$.

According to Gomory and Hu (1961), the Gomory–Hu tree can be constructed by the following procedure and can be completed with $N - 1$ time MFP number of operations.

(1) Consider the original network $G(V, A)$, an initialized iteration indicator $n = 1$, a hyper node $\mathbf{X}^{(1)}$ containing all the nodes V, an empty virtual link set $\mathbf{E}^{(1)} = \varnothing$, and undirected graph $T_1(\mathbf{X}^{(1)},\mathbf{E}^{(1)})$:
(2) Find the hypernode $X_i \in \mathbf{X}^{(n)}$ associated with two or more nodes from $\mathbf{X}^{(n)}$, and select an origin node s and destination node t from X_i;
(3) Calculate the MFP between s and t in network $G(V, A)$, and obtain the links of the minimum cut $\mathbf{a}^{(n)} \in A$ and solution of MFP λ_{st};
(4) Divide V into two subsets of nodes $S_{\mathbf{a}^{(n)}}$ and $V - S_{\mathbf{a}^{(n)}}$ by removing the links of $\mathbf{a}^{(n)}$ from $G(V, A)$. Add new hypernodes $X_p = X_i \cap S_{\mathbf{a}^n}$ and $X_q = X_i \cap (V - S_{\mathbf{a}^n})$ to $\mathbf{X}^{(n)}$;
(5) Swap the virtual links $e_{ki} \in \mathbf{E}^{(n)}$ connecting X_i as follows:

$$\left\{\begin{array}{ll} e_{ki} \to e_{kp} & \text{if } \forall k | X_k \subseteqq S_{\mathbf{a}^{(n)}} \\ e_{ki} \to e_{kq} & \text{if } \forall k | X_k \subseteqq (V - S_{\mathbf{a}^{(n)}}) \end{array}\right\}$$

(1) Remove X_i from $\mathbf{X}^{(n)}$, connect X_p and X_q via a link e_{pq} with weight λ_{st}, and add $e_{pq}$to $\mathbf{E}^{(n)}$;
(2) Update $T_n(\mathbf{X}^{(n)},\mathbf{E}^{(n)})$ and proceed to iteration number $n = n + 1$;
(3) Repeat steps 2 to 5 until $n = N$.

To illustrate this procedure, we use the test network shown in Fig. 2. Fig. 2(a) shows the link ID and capacity. First, we focus on the

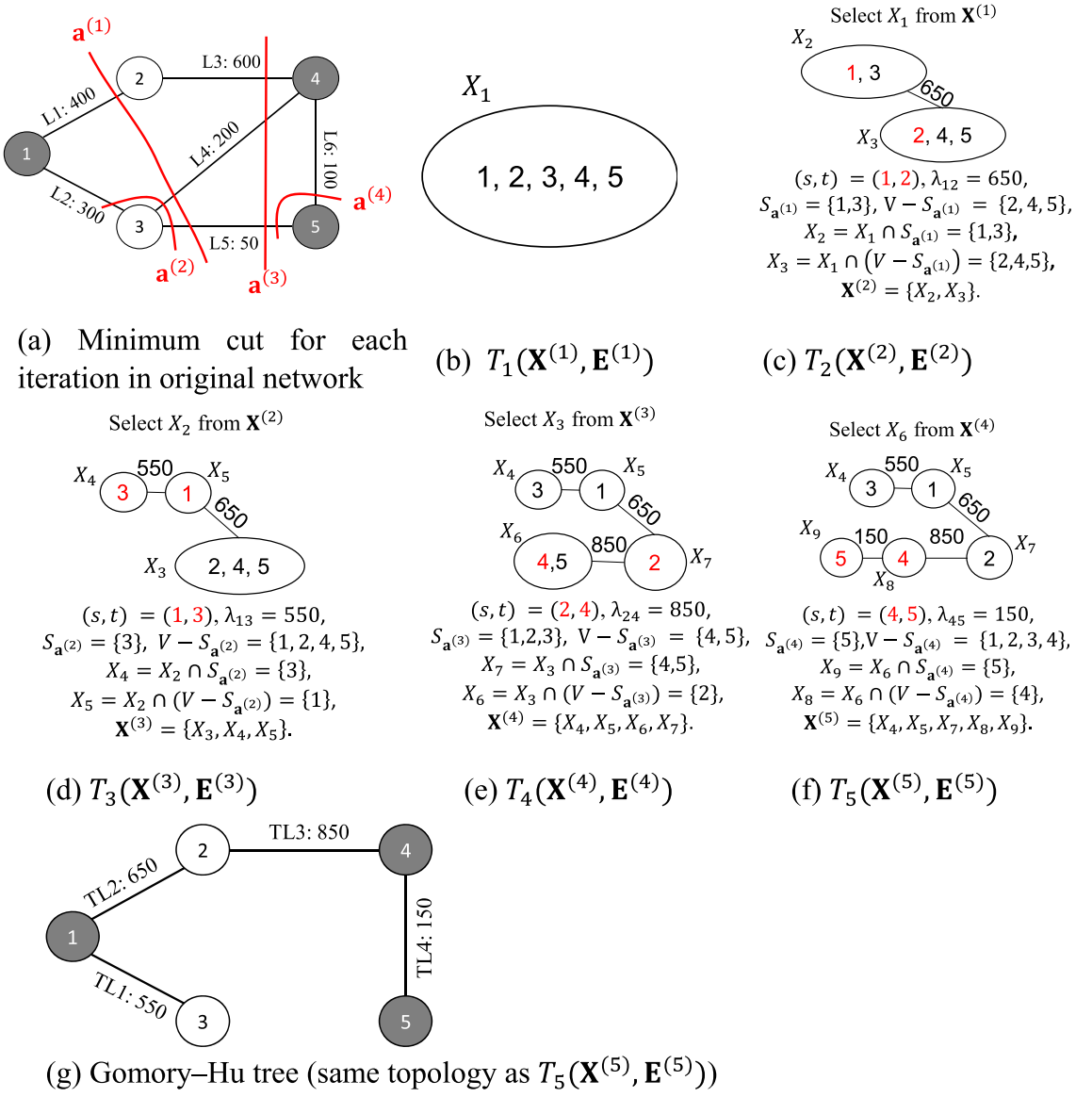

Fig. 2. Example of creating the Gomory–Hu tree for the test network.

case when $n = 1$. $T_1(\mathbf{X}^{(1)},\mathbf{E}^{(1)})$ is illustrated in Fig. 2(b) with hypernodes $X_1 = \{1, 2, 3, 4, 5\}$. Select any two nodes from X_1 (i.e., here we use (s, t) = (1, 2)). In Step 3, calculate the MFP and obtain $\lambda_{12} = 650$ and $\mathbf{a}^{(1)} = \{L1, L4, L5\}$. In Step 4, divide G into $S_{\mathbf{a}^{(1)}} = \{1,3\}$ and $V - S_{\mathbf{a}^{(1)}} = \{2, 4, 5\}$ by removing the links in cut $\mathbf{a}^1$ from $G(V, A)$; this yields $X_2 = \{1, 3\}$ and $X_3 = \{2, 4, 5\}$. Step 5 is skipped because this iteration of the tree lacks a virtual link. Completion of Steps 6 and 7 yields $T_2(\mathbf{X}^{(2)},\mathbf{E}^{(2)})$, as shown in Fig. 2(c).

In the next iteration $n = 2$, choose (s, t) = (1, 3) from X_2 in Step 2 and obtain $\lambda_{13} = 550$ and $\mathbf{a}^{(2)} = \{L2, L4, L5\}$ by calculating the MFP in Step 3. The subsets of nodes are $S_{\mathbf{a}^{(2)}} = \{3\}$ and $V - S_{\mathbf{a}^{(2)}} = \{1, 2, 4, 5\}$, and X_2 is divided into $X_4 = X_2 \cap S_{\mathbf{a}^{(2)}} = \{3\}$ and $X_5 = X_2 \cap (V - S_{\mathbf{a}^{(2)}}) = \{1\}$ in Step 4. In Step 5, swap the virtual link from e_{23} to e_{53} because of nodes $\{2, 4, 5\} \subseteq (V - S_{\mathbf{a}^{(2)}})$. T_3 can be obtained as shown in Fig. 2(d) by computing Steps 6 and 7. Similarly, T_4 can be obtained by setting $X_3 = \{2, 4, 5\}$, (s, t) = (2, 4). When iteration $n = N$, the complete Gomory–Hu tree is obtained, as shown in Fig. 2(f).

Fig. 2(g) shows the basic information provided by the Gomory–Hu tree; this includes the link weights representing the minimum cuts between the endpoints of all links. The link weight between nodes 1 and 2 (TL2) is 650, which matches the solution of the MFP between nodes 1 and 2 in the original network; the minimum cut appears in {L1, L4, L5}, and the sum of the capacities is 650 (see the first feature in the definition of the Gomory–Hu tree). For example, the solution of the MFP between node 1 and node 4 is 650, and the links belonging to the minimum cut are $\mathbf{a}_k = \{L1, L4, L5\}$. The path from node 1 to node 4 in the Gomory–Hu tree passes through {TL3, TL2}, and the respective link weights are {850, 650}. Hence, e^* is identified as TL2. The first feature shows that the minimum number of weights matches the solution of the MFP. The second feature is illustrated in Fig. 3. Two node sets $S_{\mathbf{a}_k} = \{1, 3\}$ and $V - S_{\mathbf{a}_k} = \{2, 4, 5\}$

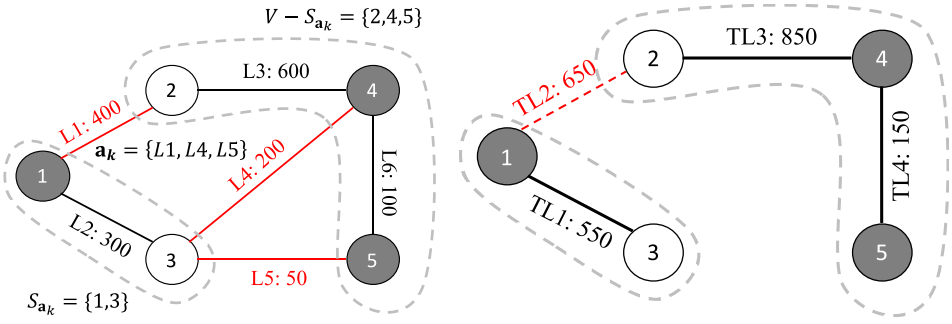

(a) Minimum cut links on the original network

(b) Two node sets created by removing TL2 from the Gomory–Hu tree

Fig. 3. Examples of the second feature of the Gomory–Hu tree.

are produced by removing $\mathbf{a}_k$ from the original network, as shown in Fig. 3(a). The pair of node sets produced by removing e^* from the Gomory–Hu tree is consistent with $S_{\mathbf{a}_k}$ and $V - S_{\mathbf{a}_k}$, as shown in Fig. 3(b). Thus, the second feature is confirmed to be valid.

As explained in Section 2.3, if two subsets of nodes are given, the passing travel demands on the cut can be obtained by Eq. (8), which quickly yields the capacity vulnerability index. The memory requirement for the links of each cut is $|A| \times |W|$ when naïvely calculating all minimum cuts for all node pairs; however, when using the Gomory–Hu tree, there is no need to retain the matrix. We next show that the passing demand for each of the $N-1$ minimum cuts can be computed using the Gomory–Hu tree topology with only network loading. Let $S_{e_{ij}}$ *and* $V - S_{e_{ij}}$ be the subsets of nodes produced by removing link $e_{ij} \in E$ from the Gomory–Hu tree $T(V, E)$; then, the following Lemma is satisfied.

Lemma 1. *For each $e_{ij} \in E$, there is a cut in the original network $G(V, A)$ with a matching subset of nodes that can be produced by removal of e_{ij}.*

Proof. From the second feature of the Gomory–Hu tree, there exists a cut $\mathbf{a}^* | (S_{e_{ij}} = S_{\mathbf{a}^*}, V - S_{e_{ij}} = V - S_{\mathbf{a}^*})$ that divides the original network into two node sets as $S_{e_{ij}}$ and $V - S_{e_{ij}}$. □

Let us denote $\mathbf{a}^*$ as the $\mathbf{a}_{e_{ij}}$ that divides V equivalently to e_{ij} via removal. Furthermore, by **Lemma 1**, the following holds.

Lemma 2. *The OD demand whose origin and destination respectively belong to $S_{e_{ij}}$ and $V - S_{e_{ij}}$ passes through $\mathbf{a}_{e_{ij}}$.*

Proof. As shown in the proof of **Proposition 1**, if an OD demand d_{st} on the original network satisfies $s \in S_{\mathbf{a}_k}, t \in (V - S_{\mathbf{a}_k})$ or $s \in (V - S_{\mathbf{a}_k}), t \in S_{\mathbf{a}_k}$ for any cut $\mathbf{a}_k$, then the demand for that OD pair passes through $\mathbf{a}_k$. From **Lemma 1**, this condition also holds for $s \in S_{e_{ij}}, t \in (V - S_{e_{ij}})$ or $s \in (V - S_{e_{ij}}), t \in S_{e_{ij}}$, and d_{st} passes through $\mathbf{a}_{e_{ij}}$. □

Furthermore, if Lemma 2 is applied to transform Eqs. (8), (9) is valid.

$$D_{\mathbf{a}_{e_{ij}}} = \sum_{s \in S_{e_{ij}}, t \in (V - S_{e_{ij}})} d_{st} + \sum_{s \in (V - S_{e_{ij}}), t \in S_{e_{ij}}} d_{st} \tag{9}$$

Eq. (9) can be applied to calculate the total demand that passes through each minimum cut of the Gomory–Hu tree method. However, with more insight, we can show that results similar to Eq. (9) can be obtained with network loading. **Lemma 3** and **Proposition 2** show that the demand passing through an arbitrary cut can be calculated by network loading onto a tree $T(V, E)$.

Lemma 3. *There is only one path between any two nodes in $T(V, E)$.*

Proof. Since the Gomory–Hu tree is a tree, there are no cyclic paths, and there can only be one path between any two nodes. □

Proposition 2. *The total demand $D_{\mathbf{a}_{e_{ij}}}$ passing through any cut $\mathbf{a}_{e_{ij}}$ can be obtained by the Eq. (10):*

$$D_{\mathbf{a}_{e_{ij}}} = \sum_{(s,t) \in W} d_{st} \delta_{e_{ij}}^{st} \quad \forall \mathbf{a}_{e_{ij}} | e_{ij} \in E \tag{10}$$

where

$$\delta_{e_{ij}}^{st} = \begin{cases} 1 & \text{if the path between } (s,t) \text{ on } T(V,E) \text{ pass through } e_{ij} \\ 0 & \text{otherwise} \end{cases}$$

Proof. Let us consider a path $\mathbf{e}_{st} = \{e_{si}, e_{ij}, \ldots, e_{nt}\}$ in $T(V, E)$ between OD pairs (s, t); $\mathbf{e}_{st}$ is unique from **Lemma 3**. Focusing on the

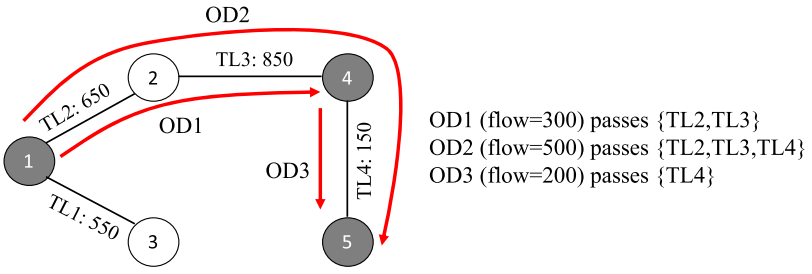

Fig. 4. Links in the Gomory–Hu tree that each OD demand passes through.

Table 4
Cut capacity and OD demand analysis of the sample network.

Link in the tree	Component of the cut	Cut capacity	Passing OD pairs	Passing OD demand
TL1	L2, L4, L5	550	–	0
TL2	L1, L4, L5	650	OD1, OD2	800
TL3	L3, L4, L5	850	OD1, OD2	800
TL4	L5, L6	150	OD2, OD3	700

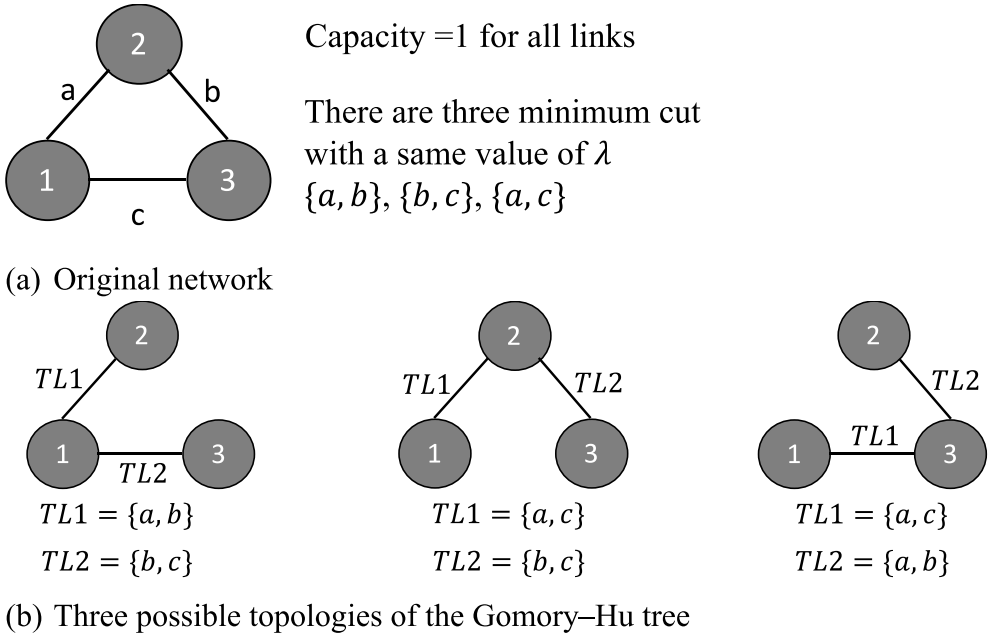

Fig. 5. Example of the Gomory–Hu tree method requiring attention.

first link of the path e_{si}, if e_{si} is removed from $T(V, E)$, (s, t) is partitioned as $S_{e_{si}} \supseteq s$, $V - S_{e_{si}} \supseteq \{i,j,\ldots,n,t\}$, and according to **Lemma 2**, the demand d_{st} must pass through $\mathbf{a}_{e_{si}}$. Similarly, if the second link e_{ij} of $\mathbf{e}_{st}$ is removed from $T(V, E)$, (s, t) is partitioned as $S_{e_{si}} \supseteq \{s,i\}$, $V - S_{e_{si}} \supseteq \{j,\ldots,n,t\}$, and the demand d_{st} passes through $\mathbf{a}_{e_{ij}}$. This result also holds for other links in $\mathbf{e}_{st}$, and we observe that d_{st} passes through the cuts $\mathbf{a}_{e_{si}}, \mathbf{a}_{e_{ij}}, \ldots, \mathbf{a}_{e_{nt}}$. Since this condition holds for $\forall(s, t) \in W$, when $d_{st} | \forall(s,t) \in W$ is sequentially loaded into the links contained in all $\mathbf{e}_{st} | \forall(s,t) \in W$, we obtain the total demand $D_{\mathbf{a}_{e_{ij}}}$ that always passes through $\mathbf{a}_{e_{ij}} | e_{ij} \in E$; this is equivalent to Eq. (10). □

This is nothing more than the result of network loading of the OD demand onto a Gomory–Hu tree. Therefore, each crossing demand of the minimum cuts of the Gomory–Hu tree can be calculated using only the topology of the tree and OD demand. Since the weight of e_{ij} is $\pi_{e_{ij}} = C_{\mathbf{a}_{e_{ij}}}$, two vulnerability indices can be obtained from the Gomory–Hu tree and OD demand.

The results obtained when applying network loading to the sample network with the OD demands listed in Table 3 are shown in Fig. 4. and Table 4.

From Fig. 4 and Table 4, we see that when the demand is loaded onto the link of the OD path, the total passing demand is obtained. For example, TL2 is passed by OD1 and OD2, and the passing OD demand = 300 + 500 = 800. This result can be equivalently obtained

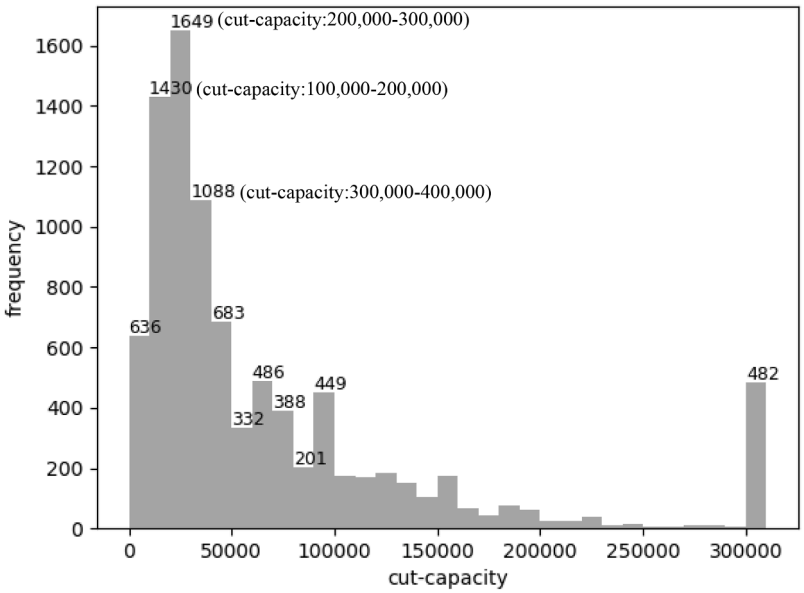

Fig. 6. Histogram of the obtained cut capacity.

with Eq. (9) (e.g., if TL2 is removed from the tree, the origin and destination of ODs 1 and 2 are partitioned to a pair of node subsets; OD 1 and 2 must hence pass through TL2).

The passing OD demand for the cut capacity ratios for TL2 and TL4 are 800/650 and 700/150, respectively. As can be seen, TL4 {L5, L6} is more congested than TL2. The reserve network capacity approach (Wong and Yang, 1997; Chen and Kasikitwiwat, 2011) finds L5 or L6; however, identification of links {L1, L4} in cut TL2 is difficult despite the OD demand exceeding the cut capacity. Our method thus reveals the relationship between the cut capacity and OD demand for all minimum network cuts.

2.5. Notes on the Gomory–Hu tree method

Note that the Gomory–Hu tree is not a unique graph; the topology varies according to the choice between the two nodes in step 2 of creating the Gomory–Hu tree. In particular, several minimum cuts may have the same λ value. Fig. 5 shows three topologies for the same graph, with each tree lacking one of the minimum cuts in the graph.

This issue may not often arise in practice because the link capacities vary widely; nevertheless, additional analysis can resolve any problems. All links included in multiple minimum cuts with the same lambda are identified as links activated in the capacity constraints of the MFP solution. Therefore, the analyst can obtain all minimum cuts for the OD pairs that require attention (with small cut-capacity or larger capacity vulnerability) by calculating additional MFPs.

3. Application to a large-scale road network

In this section, we present an application of the proposed method to study a large road network in central Japan, as shown in Fig. 8. The network includes 18,051 links (39,885 km), 12,007 nodes, 1049 centroids, and 182,263 OD pairs. This network includes a wide range of land uses, including urban, mountainous, coastal area etc. The links include expressways, national highways, and prefectural roads, covering all major trunk roads. Hence, this network is appropriate for identifying vulnerable places and analyzing their characteristics because it includes a large variation in land use patterns and road density.

Using the Gomory–Hu method, we found that many cuts were possible for links connected to the origin or destination nodes. In general, if there are many alternative paths between an origin and a destination, the capacity of the cut that is farthest from the origin or destination node will be large; the minimum cut can potentially be determined by links connected to the origin or destination. To identify the vulnerable cuts between the OD pairs, we revised the network topology. The origins and destinations are nodes of the network; however, the real travel demand lies in zones closest to such nodes. Thus, we added high-capacity pseudo-links with 300,000 capacity between the origin/destination nodes and their adjacent nodes. We applied the Gomory–Hu tree method via Python using the "python-igraph" library; the task required less than 3 min on a personal computer using Windows 10 with an AMD Ryzen 3800x CPU and 64 GB of DDR4-3200 RAM. Therefore, the method can be applied to a real, large-scale transportation network without any computational issues. A histogram of the obtained connectivity-vulnerability index is shown in Fig. 6, and a scatter plot of the ratio of capacity to crossing demand for the capacity-vulnerability index is shown in Fig. 7.

The number of obtained minimum cuts is 12,006, which is equal to the number of nodes in the graph minus one (i.e., $N - 1$), because it follows the features of a tree graph. The most frequent value of connectivity vulnerability are between 20,000 and 30,000,

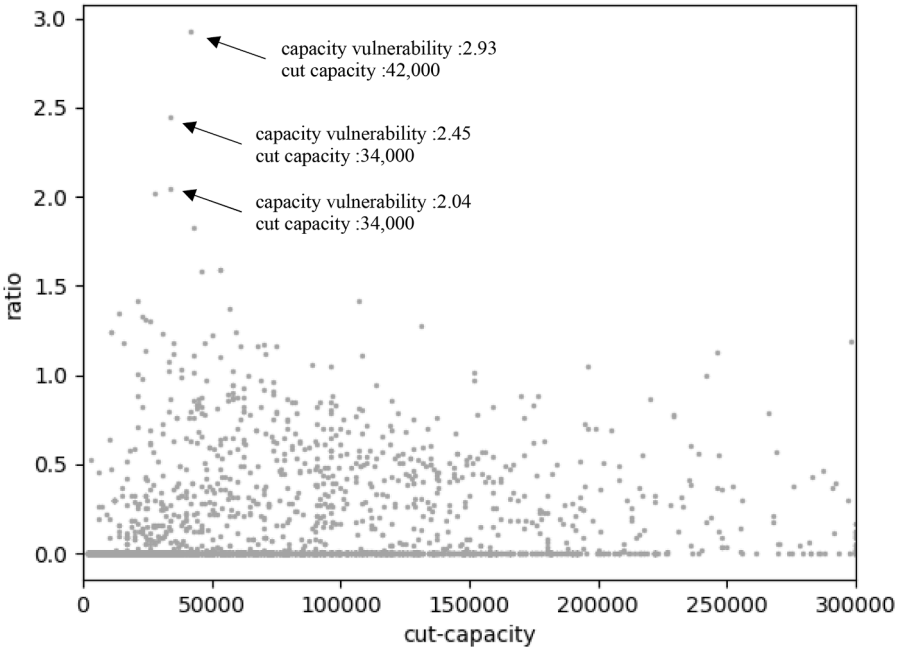

Fig. 7. Scatter plot of the cut capacity and ratio of crossing demand to cut capacity.

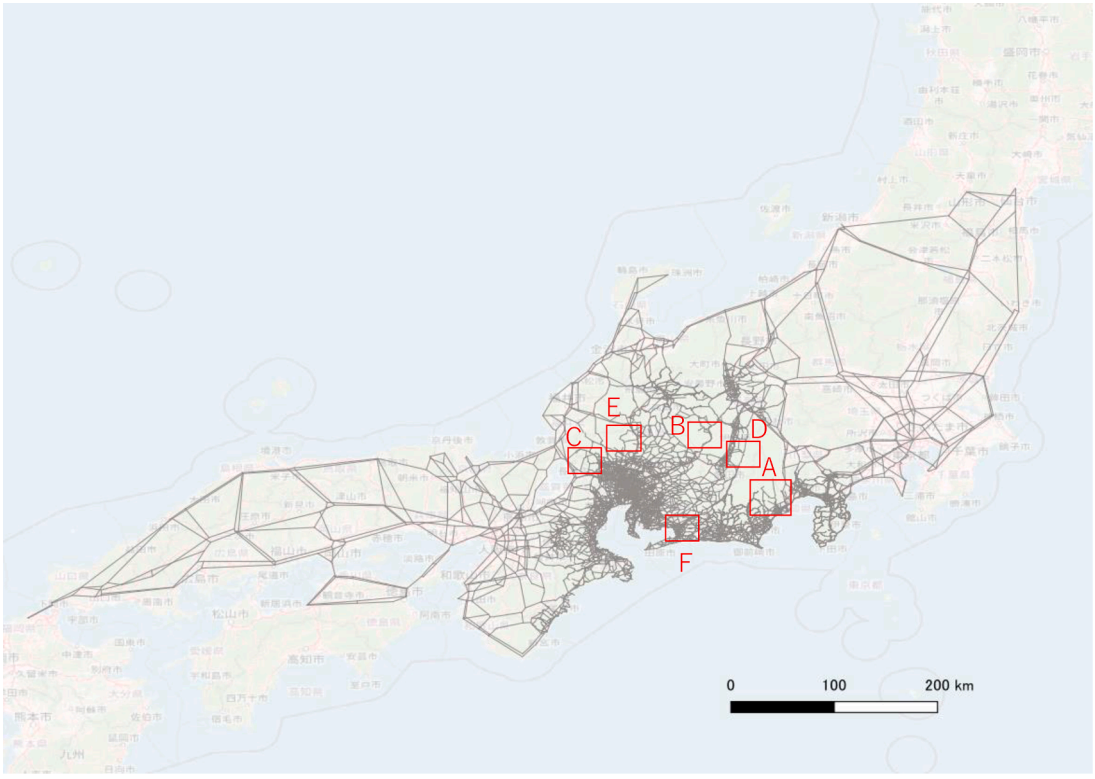

Fig 8. Road network of central Japan and the locations of 10 small capacity cuts.

and there are 1649 cuts in this range. The number of larger connectivity-vulnerability cuts decreases rapidly. Since the capacity of all the links connecting the origin/destination nodes was set to 300,000, and 482 cuts with large values of cut capacity are affected by the added pseudo links.

Table 5
Data on small connectivity-vulnerable cuts.

Rank	ID	Cut capacity (connectivity vulnerability)	Demand	Capacity vulnerability	Area
1	1-a “Igawa”	3000	1582	0.53	A
2	2-b “Kuchisakamoto”	6000	1582	0.26	A
2	2-c “Okawa”	6000	1171	0.20	A
2	2-d “Kuchisakamoto-Okawa”	6000	2753	0.46	A
5	5-e “Otaki”	7000	1842	0.26	B
6	6-f “Kasuga”	9000	1984	0.22	C
7	7-g “Kuchisakamoto-Katsuragawa”	10,000	6438	0.64	A
7	7-h “Oshika”	10,000	907	0.09	D
7	7-i “Itadori”	10,000	1957	0.20	E
10	7-j “Toyohashi”	11,000	5167	0.47	F

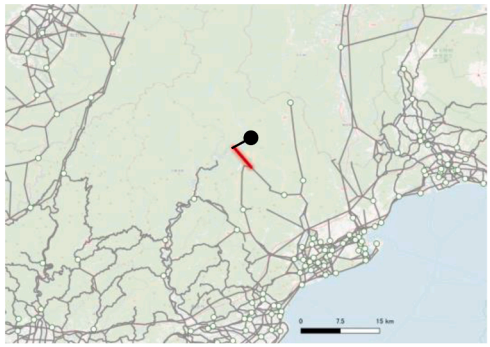

(a) 1-a “Igawa”

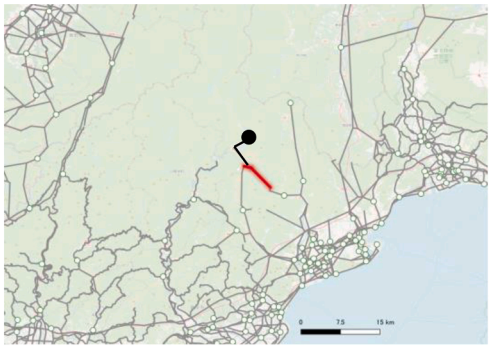

(b) 2-b “Kuchisakamoto”

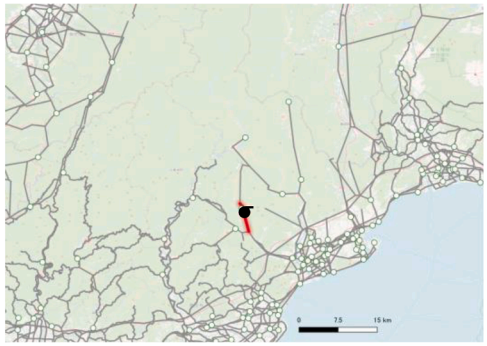

(c) 2-c “Okawa”

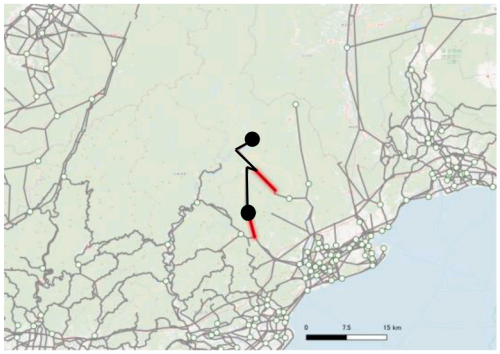

(d) 2-d “Kuchisakamoto-Okawa”

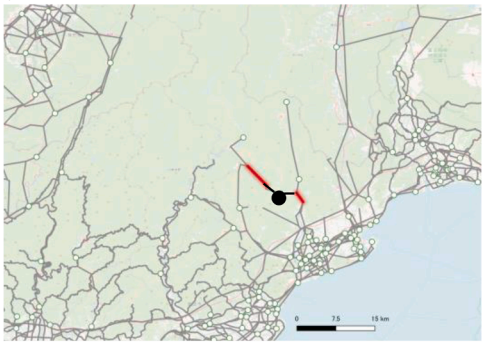

(e) 7-g “Kuchisakamoto-Katsuragawa”

Fig. 9. Links among the minimum cuts of area A.

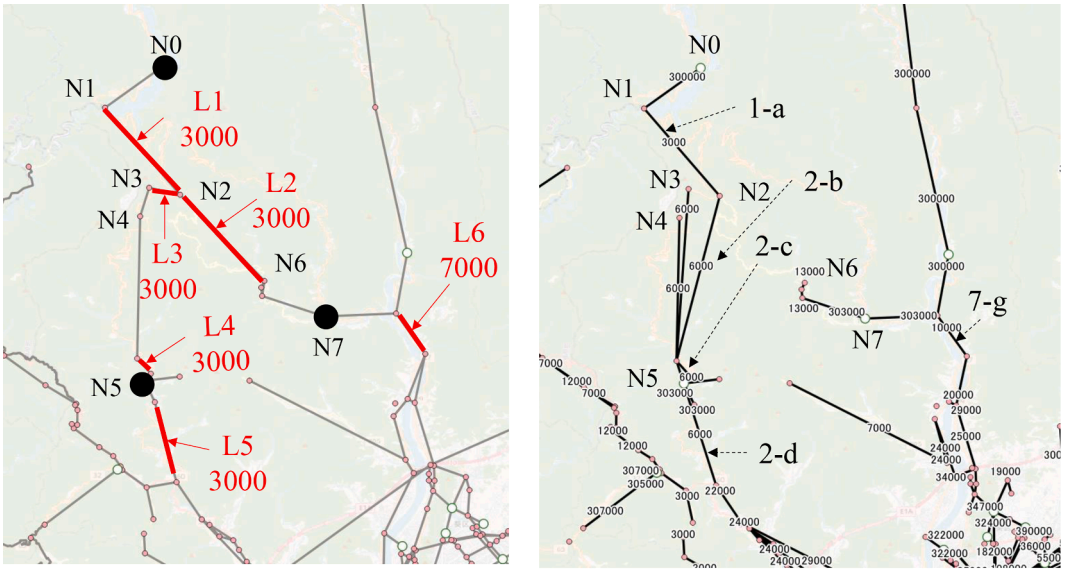

(a) Original network *(b) Gomory–Hu tree*

Fig. 10. Comparison of the original network and the Gomory–Hu tree.

Table 6
Checking for consistency of the Gomory–Hu tree features.

Cut link in Gomory–Hu tree	Cut links in original network(link capacity)	Separated origin/destinationnodes (OD demand from/to the node)
1-a "Igawa"	L1(3000)	N0(1582)
2-b "Kuchisakamoto"	L2(3000), L3(3000)	N0(1582)
2-c "Okawa"	L4(3000), L5(3000)	N5(1171)
2-d "Kuchisakamoto -Okawa"	L2(3000), L5(3000)	N0(1582), N5(1171)
7-g "Kuchisakamoto -Katsuragawa"	L2(3000) L6(7000)	N7(6438)

The maximum capacity vulnerability is therefore 2.93, and the figure shows that cuts with large values can be vary independent of connectivity vulnerabilities. On the other hand, the number of cuts with zero capacity vulnerability is 10,314, which indicates that the origin/destination node is not included in any of the subgraphs divided by the cuts.

Numerous cuts with zero crossing demands are seldom used in practice and lie at the edge of network; hence, they have minimal effects on road maintenance/construction policies. We therefore included only the minimum cuts with non-zero crossing demands. Ten smaller cuts and their properties are shown in Fig. 8 and Table 5. The smaller cuts appear in six areas shown in red boxes; Fig. 9 shows five cuts in the area A.

The red lines are the links between the minimum cuts; the thick lines and black circles are the separated links and the origins and destinations that are divided from other components of network by the cut. All cuts in area A shown in Fig. 9 are at the edges of the network in a mountainous area with few roads. This is reasonable because the path diversity is low, and the cut capacity values range from 3000 to 10,000. As the origins or destinations of areas with such low cut capacities are greatly affected by external forces after a disaster, the road administrators should aim to improve the physical robustness of these roads and construct new roads to increase the number of alternative paths. However, residents and businesses must prepare for long periods of isolation; time and money are needed to improve the cut capacity in an area with many minimum cuts with low cut capacities.

The Gomory–Hu tree for this area is shown in Fig. 10. The red text shows the link ID and link capacity. We now explore the features of the tree focusing on node N0 of Fig. 10(b). After removal of tree link *1-a*, nodes N0 and N1 are separated from the other nodes. As all paths between N0 and all origins/destinations pass through a link in *1-a "Igawa"*, the minimum cut value for N0 and all origins/destinations is 3000 (the capacity of "L1"). To separate N1 and N0 from the other nodes in the original network, the link "L1" connecting N1 and N2 must be removed, consistent with the link shown in Fig. 10(a). Similarly, N0, N1, and N2 are separated from other nodes if link *2-b* "Kuchisakamoto" is removed from the tree; the cut link is shown in Fig. 10(b), and the corresponding capacity is 6000. This link is consistent with "L2" and "L3" in the original network shown in Fig. 10(a). When *1-a "Igawa"* or *2-b "Kuchisakamoto"* is removed from the network, only N0 is separated in the origin/destination node, so the crossing demand is 1582; this number is obtained as the OD demand from/to N0. When *2-c* "Okawa" is removed, N5 is separated, and the crossing demand is 1171 and obtained as

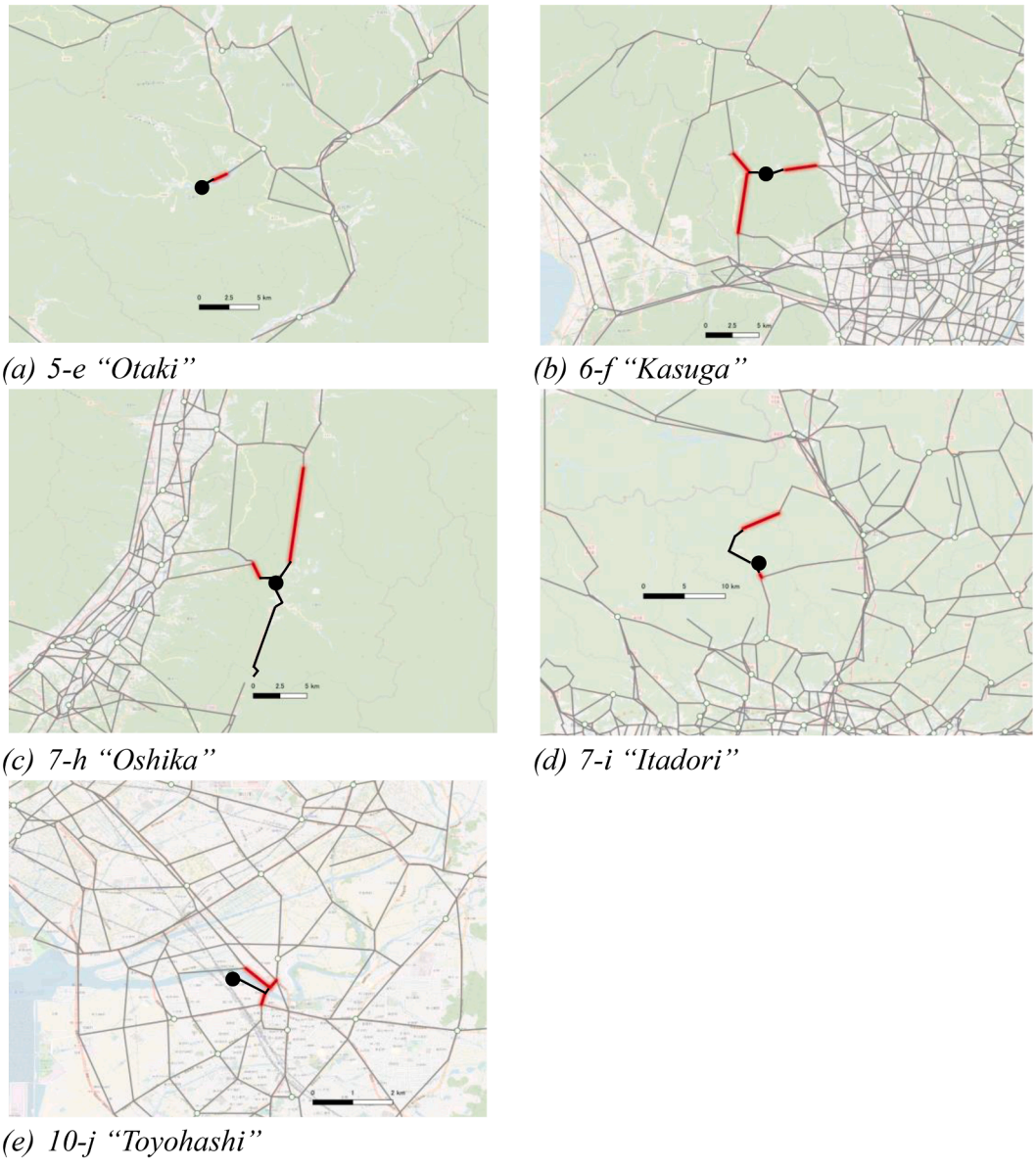

Fig. 11. Ten cuts outside area A that exhibit high connectivity vulnerability.

the OD demand from/to N5. Similar to these, the cut on the Gomory–Hu tree, the cut links of the original network, and the origin/destination nodes that are separated when the cut is removed, are organized as shown in Table 6.

We can confirm the consistency of the features of the Gomory–Hu tree by these results.

The cuts in areas other than area A are shown in Fig. 11.

Many of these cuts lie in mountainous areas with sparse roads; however, 10-j (Toyohashi) is in an urban area close to a river. Only a few bridges cross the river, and only one road connects to the centroid node. It should be noted that connectivity-vulnerable cuts may occur even in urban areas where the links tend to be sparse, such as near a river. As shown in Table 5, 10 small-capacity cuts do not have large crossing demands. Therefore, they may not pose major problems during evacuation after a disaster if the links are not degraded by external forces. Fig. 12 shows the locations of 10 large capacity-vulnerable cuts, and Table 7 summarizes the attributes of these cuts.

The capacity vulnerability values range from 1.41 to 2.93. Both capacity and demand are defined based on data from a single day, suggesting that the cuts are often congested. In terms of the cut locations, five cuts (Ranks 1–4, and 8) are near the sea and associated with tsunami risks. Evacuation during a tsunami would lead to many casualties if these cuts are congested. Therefore, the evacuation plans must include both the provision of facilities and evacuation without using vehicles. The Rank 5 cut lies inside the Rank 10 cut of a hot spring area visited by many tourists. The capacity of the Rank 10 cut is greater than the highest rank cut of 107,000; however, the

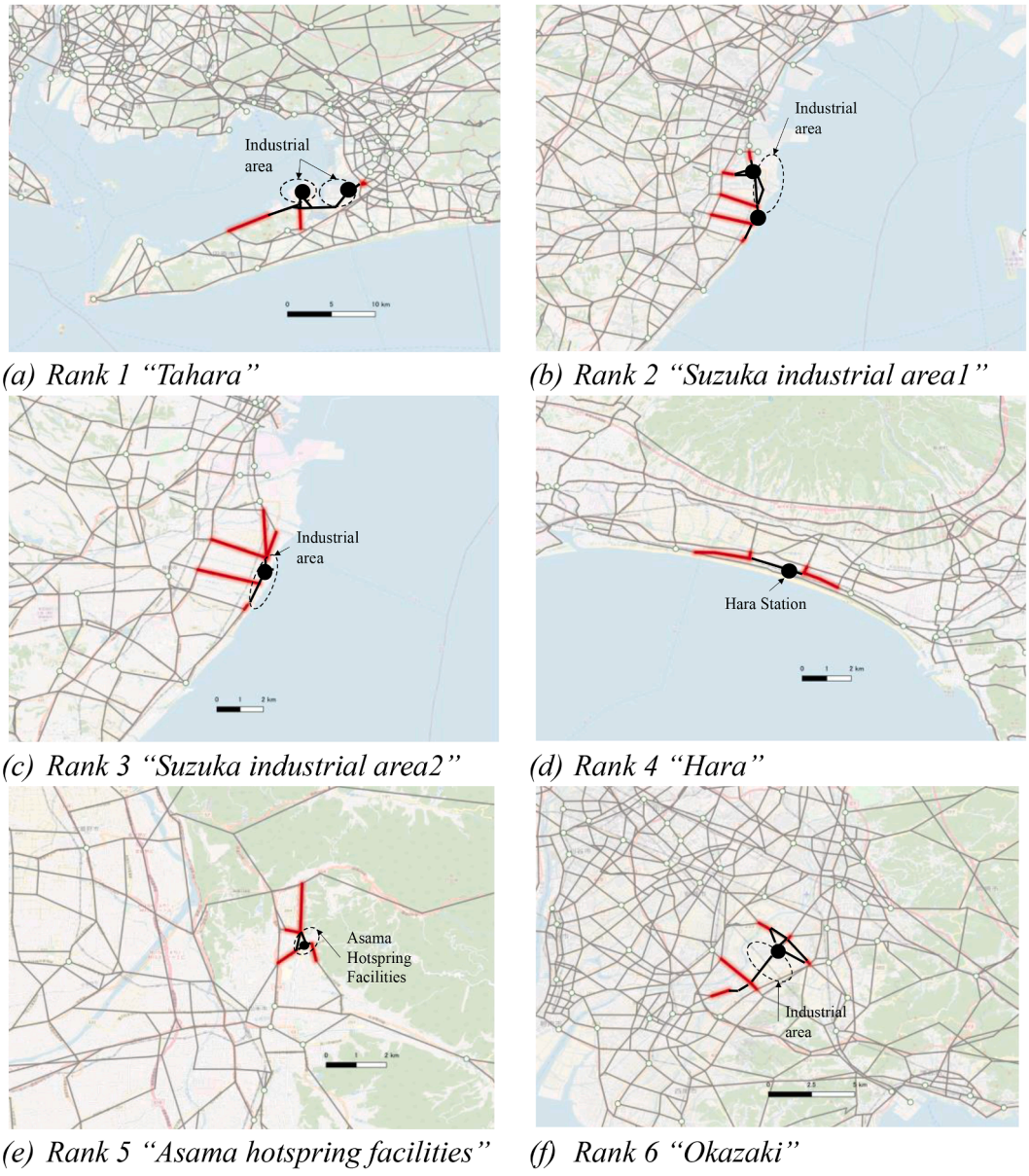

Fig. 12. Ten high-capacity vulnerable cuts in the target road network.

crossing demand exceeds this value. Most of these high-capacity vulnerable cuts are located in mountainous sightseeing areas and industrial areas near the sea, where the road network is sparse and many employees and tourists visit. Hence, these cut locations with high-capacity vulnerabilities are intuitive, and the results are reasonable. However, the cuts of these complex links may not be obvious even to experienced road administrators; therefore, our method yields useful information to help road administrators manage the road networks in their jurisdictions.

The relationship between the road hierarchy, high-capacity vulnerable cuts, and the link capacity contained in these cuts was analyzed. Figure 13 shows the distribution of link capacity in the applied network. Table 8 shows capacity of the links in high-capacity vulnerable cuts. All the links included in the high-capacity vulnerable cuts have a capacity less than 15,000, and Expressway is not included. The number of links in each cut is between 4 and 6, except for cuts of Rank 7 and 10. Hence, adding links inside and outside these cut areas can be expected to increase the capacity of the cuts. Using Suzuka city as an example with high-capacity vulnerable cuts, adding high-level roads such as expressway can be expected to efficiently improve the capacity of the minimum cut and reduce the vulnerability of areas connecting to Suzuka city. On the other hand, if it is not cost-effective to construct new roads in this area (e.g., mountainous region), strategies to reduce the demand should be considered (e.g., evacuation transportation by bus).

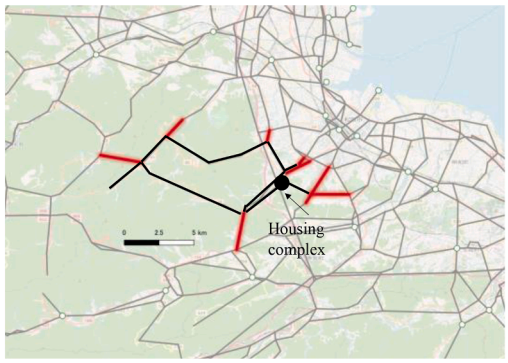

(g) Rank 7 "Suzuka housing area"

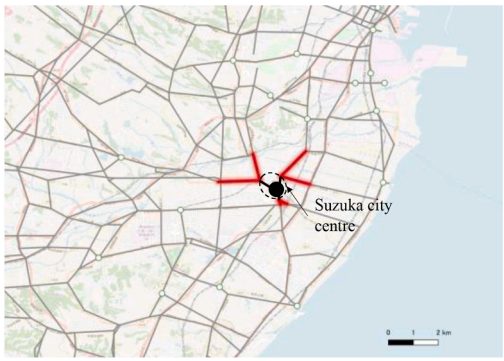

(h) Rank 8 "Suzuka city centre"

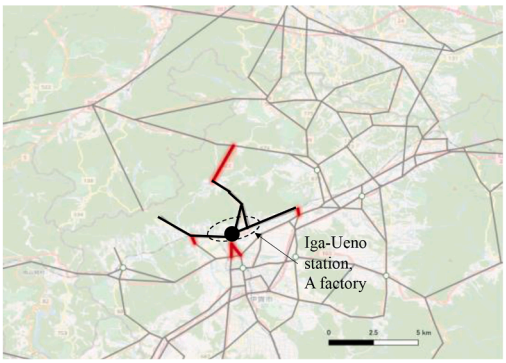

(i) Rank 9 "Iga-Ueno"

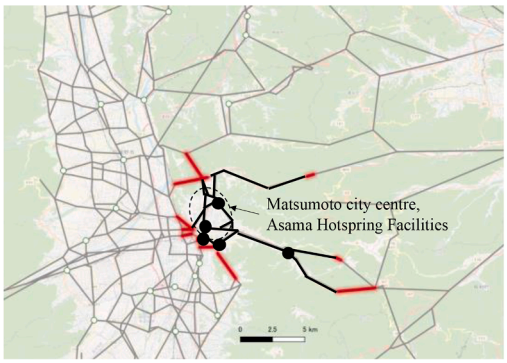

(j) Rank 10 "Asama hotspring facilities"

Fig. 12. (*continued*).

Table 7
High-capacity vulnerable cuts.

Rank	Location	Cut capacity (connectivity vulnerability)	Demand	Capacity vulnerability
1	Tahara city	42,000	123,080	2.93
2	Suzuka city	34,000	83,221	2.45
3	Suzuka city	34,000	69,381	2.04
4	Numazu city	28,000	56,558	2.02
5	Matsumoto city	43,000	78,359	1.82
6	Okazaki city	53,000	84,402	1.59
7	Suzuka city	53,000	84,224	1.59
8	Suzuka city	46,000	72,927	1.59
9	Iga-Ueno city	21,000	29,778	1.42
10	Matsumoto city	107,000	151,234	1.41

4. Conclusion

We present a unified method for analyzing both connectivity and capacity vulnerabilities without any route-choice assumptions; we used the Gomory–Hu tree method to efficiently calculate the vulnerable cuts. Both vulnerability indices provided vulnerability cuts that consisted of multiple links. The proposed method shows that the demand crossing the minimum cut for each pair of nodes in the network can be obtained by network loading of the Gomory–Hu tree. We then applied our proposed method to a road network with over 18,000 links, 12,000 nodes, and 180,000 OD pairs. In less than 3 min of computational time, the method yielded all the required outputs. In terms of capacity vulnerability, the more vulnerable cuts were found to be around the edge of the network. Although the crossing demands for these cuts were typically small, they may increase greatly if the links on the cut are damaged by a disaster, as there are often no alternative paths. On the other hand, the capacity-vulnerable cuts lie in industrial and sightseeing areas frequented by many employees and tourists, where the path diversity is often limited. If the demand to cut-capacity ratio is greater than 1, congestion may be a chronic problem, particularly after a disaster. Five of the top ten capacity-vulnerable cuts lie near the sea and must be considered when planning for tsunami evacuations. In such cases, it may be necessary to forego the use of vehicles and instead evacuate people inland via emergency high-speed railways.

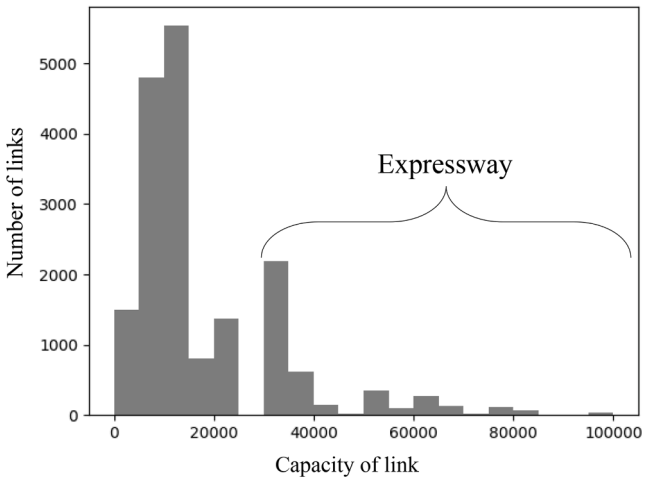

Fig. 13. Histogram of link capacity.

Table 8
Capacity of the links in high-capacity vulnerable cuts.

Rank	Location	Number of links	Number of links with capacity grade			
			$\leq$ 5000	$\leq$ 10, 000	$\leq$ 15, 000	$\leq$ 20, 000
1	Tahara city	4		3	1	
2	Suzuka city	5	2	1	2	
3	Suzuka city	5	2	1	2	
4	Numazu city	4		4		
5	Matsumoto city	4		1	3	
6	Okazaki city	6		5	1	
7	Suzuka city	9	3	5	1	
8	Suzuka city	6	2	3	1	
9	Iga-Ueno city	4	1	3		
10	Matsumoto city	11	1	5	5	

5. Discussion

In the real-world application, the network that we evaluated principally features arterial roads and ignores narrow streets. The capacity vulnerability of a cut may not be small when we use the detailed road network, including all minor streets, (especially in urban areas, the minimum cuts may change dramatically due to the densities of the minor streets). However, the computation time may increase if the number of components in the network increase owing to inclusion of all the minor streets; thus, policymaking requires that the appropriate settings are chosen. If a vulnerable cut is identified in an arterial road network, it can be validated by reanalyzing the vulnerability for a detailed subnetwork, including the minor streets around the vulnerable cut. The vulnerability evaluations also depend on origin/destination node choices; this also requires careful preplanning.

The difference between capacity and crossing demands may reveal excess demand; if the difference is large, this issue may need to be addressed even if the ratio is small. We thus recommend that both differences and ratios be calculated when seeking to improve a network. The OD data used in the application is obtained from a national survey that observes the daily demands under normal conditions. Transportation demand for commuting to work/school is expected to behave similarly during an evacuation since the route travels back and forth between residences and workplaces/schools; however, this may not be completely consistent with evacuation demands.

As shown in Fig. 7, which evaluates the connectivity vulnerability and capacity vulnerability for the same cut, there is no direct correlation. Therefore, we believe that the two indicators can be separately used depending on the availability of demand information. For instance, a cut with an extremely small connectivity vulnerability can easily cause congestion if the heavy demand concentrates on it unexpectedly. Therefore, it would be necessary to increase the cut capacity of an extremely small connectivity vulnerability. On the other hand, capacity vulnerability provides the ratio of demand to capacity of the cut (i.e., similar to demand and supply) that can be used to investigate not only investments in roads to increase the cut capacity, but also policies to distribute emergency evacuation demand to other transport modes.

In this study, we computed the minimum cut between all pairs of nodes in the network and calculated the vulnerability index for each minimum cut; however, in the application, the analysis focuses only on cuts where the demand crosses a set value. If only the cuts through which the demand passes are required for the result, the tree to be constructed for the analysis only needs to represent the minimum cuts between the origin and destination nodes. Therefore, if the method to generate trees focusing only on the origin/

destination nodes in the network is constructed and the proposed vulnerability index is provided, equivalent results may be obtained with fewer operations. We intend to develop this method further in a future study.

CRediT authorship contribution statement

Satoshi Sugiura: Conceptualization, Funding acquisition, Methodology, Software, Writing – original draft, Writing – review & editing. **Anthony Chen:** Conceptualization, Funding acquisition, Methodology, Writing – review & editing, Supervision.

Declaration of Competing Interest

None.

Acknowledgments

This research was jointly supported by the National Natural Science Foundation of China (Project No. 72071174), the Research Grants Council of the Hong Kong Special Administrative Region (Project No. 15267116), the Hong Kong Branch of National Rail Transit Electrification and Automation Engineering Technology Research Center (K-BBY1), the Committee on Advanced Road Technology under the authority of the Ministry of Land, Infrastructure, Transport, and Tourism in Japan (Project name "Research on the evaluation of spatial economic impacts of building bus termini", Principal Investigator: Prof. Yuki Takayama, Kanazawa University).

References

Bell, M.G.H., 2000. A game theory approach to measuring the performance reliability of transport networks. Transp. Res. Part B 34 (6), 533–545.
Bell, M.G.H., Kurauchi, F., Perera, S., Wong, W., 2017. Investigating transport network vulnerability by capacity weighted spectral analysis. Transp. Res. Part B 99, 251–266.
Berdica, K., 2002. An introduction to road vulnerability: what has been done, is done and should be done. Transp. Policy 9 (2), 117–127 (Oxf).
Chen, A., Kasikitwiwat, P., 2011. Modeling network capacity flexibility of transportation networks. Transp. Res. Part A 45 (2), 105–117.
Chen, A., Yang, C., Kongsomsaksakul, S., Lee, M., 2007. Network-based accessibility measures for vulnerability analysis of degradable transportation networks. Netw. Spat. Econ. 7, 241–256.
D'Este, G.M., Taylor, M.A.P., 2001. Modelling network vulnerability at the level of the national strategic transport network. J. East. Asia Soc. Transp. Stud. 4 (2), 1–14.
D'Este, G.M., Taylor, M.A.P., 2003. Network vulnerability: an approach to reliability analysis at the level of national strategic transport networks. In: Bell, M.G.H., Iida, Y. (Eds.), The Network Reliability of Transport. Pergamon Press.
Du, M., Jiang, X., Cheng, L., 2017. Alternative network robustness measure using system-wide transportation capacity for identifying critical links in road networks. Adv. Mech. Eng. 9 (4), 1–12.
Faturechi, R., Miller-Hooks, E., 2015. Measuring the performance of transportation infrastructure systems in disasters: a comprehensive review. J. Infrastruct. Syst. 21 (1), 04014025.
Gomory, R.E., Hu, T.C., 1961. Multi-terminal network flows. SIAM J. Appl. Math. 9, 551–570.
Goldberg, A.V., Tarjan, R.E., 1988. A new approach to the maximum-flow problem. J. Assoc. Comput. Mach. 35 (4), 921–940.
Ho, H.W., Sumalee, A., Lam, W.H.K., Szeto, W.Y., 2013. A continuum modeling approach for network vulnerability analysis at regional scale. Soc. Behav. Sci. 80, 846–859.
Jenelius, E., Petersen, T., Mattsson, L.G., 2006. Importance and exposure in road network vulnerability analysis. Transp. Res. Part A 40, 537–560.
Kurauchi, F., Uno, N., Sumalee, A., Seto, Y., 2009. Network evaluation based on connectivity vulnerability. In: Proceedings of the 18th International Symposium on Transportation and Traffic Theory, pp. 637–649.
Matisziw, T.C., Murray, A.T., 2009. Modeling s-t path availability to support disaster vulnerability assessment of network infrastructure. Comput. Oper. Res. 36, 16–26.
Mattsson, L.G, Jenelius, E., 2015. Vulnerability and resilience of transport systems –a discussion of recent research. Transp. Res. Part A 81, 16–34.
Murray-Tuite, P.M., Mahmassani, H.S., 2004. Methodology for the determination of vulnerable links in a transportation network. Transp. Res. Rec. 1882, 88–96.
Nagurney, A., Qiang, Q., 2007. A network efficiency measure for congested networks. Europhys. Lett. 79 (38005), 1–5.
Scott, D.M., Novak, D.C., Aultman-Hall, L., Guo, F., 2006. Network robustness index: a new method for identifying critical links and evaluating the performance of transportation networks. J. Transp. Geogr. 14, 215–227.
Taylor, M.A.P., 2008. Critical transport infrastructure in urban areas: impacts of traffic incidents assessed using accessibility-based network vulnerability analysis. Growth Change 39 (4), 593–616.
Taylor, M.A.P., 2017. Vulnerability Analysis for Transportation Networks. Elsevier, Oxford.
Taylor, M.A.P., Susilawati, 2012. Remoteness and accessibility in the vulnerability analysis of regional road networks. Transp. Res. Part A 46, 761–771.
Tatano, Y., 2017. Toward the quantification of the resilience of the road network. Expressways Automob. 60 (9), 5–8 (in Japanese).
Wong, S.C., Yang, H., 1997. Reserve capacity of a signal-controlled road network. Transp. Res. Part B 31 (5), 397–402.
Xu, X., Chen, A., Jansuwan, S., Yang, C., Ryu, S., 2018. Transportation network redundancy: complementary measures and computational methods. Transp. Res. Part B 114, 68–85.